The Effect of Thermal Boundary Conditions and Scaling on Electro-Thermal-Compliant Micro Devices

Nilesh Mankame and G. K. Ananthasuresh

Mechanical Engineering and Applied Mechanics
University of Pennsylvania, Philadelphia, PA 19104-6315
{nileshdm, gksuresh}@seas.cis.upenn.edu

ABSTRACT

Electro-thermal micro actuators that operate by virtue of constrained thermal expansion induced by Joule heating, have recently received considerable attention. We use electro-thermal actuation to create monolithic compliant devices with embedded actuation in which the actuator and the mechanism are indistinguishable. These devices can be made at micro (micron size) or meso (hundreds of microns to a millimeter size) scales using any conducting material. In this paper, we examine the scaling effects on these devices, and also present a comparative study of essential and natural boundary conditions used in the thermal analysis. The experimental data and the results of comprehensive analysis that includes conduction through the substrate and the air-gaps; convection; and radiation, are used to make some observations that are generally applicable to electro-thermal-compliant micro devices.

1 INTRODUCTION

The operating principle of electro-thermal micro actuators is the constrained thermal expansion of a flexible continuum of material as a result of Joule heating. Recently, these actuators have received considerable attention [1-7]. Embedded electro-thermal-compliant (ETC) actuation, a generalization of the *basic electro-thermal actuator* concept of [1, 2], fully integrates the mechanism and the actuator with an appropriate shape [3, 4] (see Figs. 1 - 4). The three degree-of-freedom planar, parallel micromanipulator in Fig. 3c can be positioned and oriented arbitrarily within a limited workspace by changing the voltage potentials at its three electrodes. Fig. 4 is an example where we used selective doping to vary resistivity within the structure to enhance differential thermal expansion. Thus, not only the shape but also the non-uniform resistivity can provide desired deformation of ETC devices.

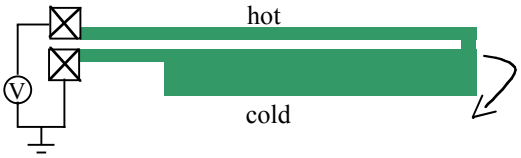

Fig. 1a Series electro-thermal actuator [1, 2]

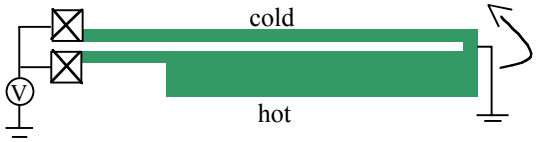

Fig. 1b Parallel electro-thermal actuator [3, 4]

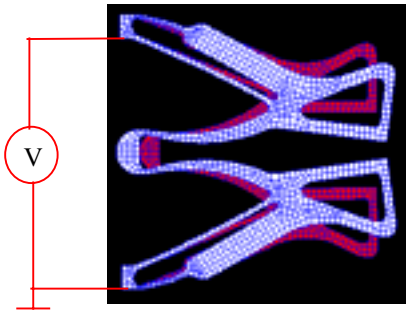

Fig. 2 A gripper with embedded ETC actuation

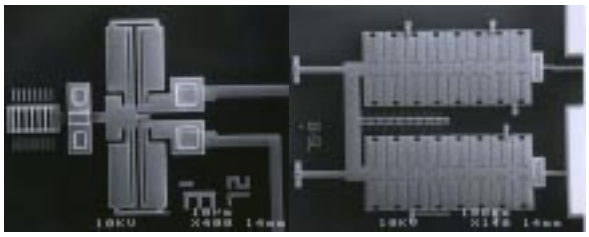

Fig. 3a ETC expansion building block; 3b An ETC linear actuator using an array of 3a

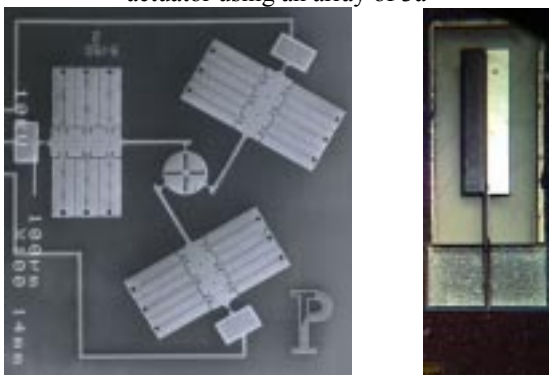

Fig. 3c Three degree-of-freedom ETC parallel manipulator
Right: Fig. 4 Selectively doped ETC actuator

The ETC devices can be made with any conducting material at any scale. However, practical considerations on maximum current, maximum voltage, consumed power, maximum temperature, etc., limit their use to micro (micron size) and meso (hundreds of microns to a few millimeters) scales. Changing electrical, thermal, and mechanical boundary conditions can significantly alter the performance of ETC devices. Electrical boundary conditions determine how the device is actuated. Mechanical boundary conditions control how the device is constrained from movement. Both electrical and mechanical conditions can be considered unchanging for a given ETC device. Thermal boundary conditions (conduction, convection, and radiation), on the other hand, depend on the environment, how the device is mounted, surface quality, etc. Therefore, careful modeling of thermal boundary conditions is necessary for the correct theoretical prediction of the behavior of ETC devices.

In this paper, the effects of thermal boundary conditions and scale on ETC devices are discussed.

2 SIMULATION OF ETC DEVICES

2.1 Governing equations

The steady-state simulation of the devices with embedded ETC actuation entails the sequential solution of three sets of differential equations that govern the electric current, thermal, and thermo-elastic behaviors. First, the current distribution in the structure for specified voltage boundary conditions is determined by solving the following equation for continuity of current [8]:

$$\vec{\nabla} \cdot \vec{J} + i_v = 0 \qquad (1)$$

where

i_v = current source per unit volume

$\vec{J}$ = conduction current density vector = $\frac{1}{\rho}\vec{E}$

ρ = electrical resistivity

$\vec{E}$ = electric field intensity = $-\vec{\nabla}V$

V = electric potential (voltage)

With no current source ($i_v = 0$), for a homogeneous medium (ρ is constant) Equation 1 simplifies to

$$\nabla^2 V = 0 \text{ and boundary conditions on } V \qquad (2)$$

whose solution gives voltage and current distributions within the structure. After obtaining the current distribution, non-uniform Joule heating is computed as follows.

Joule heat generation rate per unit volume is

$$\dot{q} = \vec{J} \cdot \vec{E} = \rho \left\| \vec{J} \right\|^2 \qquad (3)$$

which for a uniform conductor reduces to the familiar $i^2 R$ form where i is current and R is the resistance. Using $\dot{q}$ as the heat source, in the second step of the simulation, the steady-state heat conduction equation shown below is solved for temperature distribution for specified thermal boundary conditions on temperature and heat flux (including insulation, natural convection, and radiation).

$$k \nabla^2 T + \dot{q} = 0 \qquad (4)$$

where T is the temperature, k is the thermal conductivity, and heat flux = $-k\vec{\nabla}T$. The third and final step in the simulation is to solve the elastic equilibrium equations under temperature induced thermal strain.

$$\vec{\nabla}\vec{\sigma} = \vec{0} \qquad (5)$$

with

$\vec{\sigma}$ = stress = $\vec{\vec{D}}\left(\vec{\varepsilon} - \vec{\varepsilon}_t\right)$

$\vec{\vec{D}}$ = elasticity tensor that relates stress and strain

$\vec{\varepsilon}_t$ = thermal strain; for plane-stress conditions, $\vec{\varepsilon}_t = \left[\alpha(T - T_0) \quad \alpha(T - T_0) \quad 0\right]^T$

T_0 = reference temperature

and conditions of specified displacements on the boundary.

2.2 Thermal boundary conditions

It should be noted that accurate thermal analysis that includes the conduction, convection, and radiation effects, is essential to correctly predict the behavior of ETC devices. Not only quantitative but also qualitative behavior can change if thermal boundary conditions are not modeled correctly. An example of a device [7] that exhibits markedly different behavior with and without modeling the convection and radiation is shown in Figs. 5a and 5b.

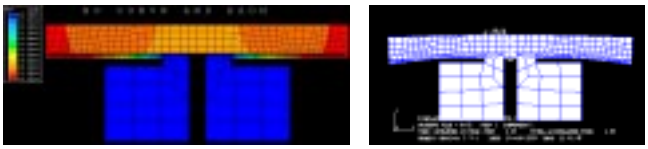

Figs. 5a Simulated temperature and deflection of an ETC device without modeling convection and radiation

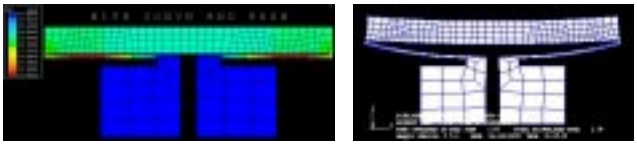

Fig. 5b Simulated temperature and deflection of the same device with convection and radiation

Thermal analysis of micro-devices in the literature has focused on applications where the anchored base pads of

the device can be assumed to be thermally grounded. Under these conditions for a limited range of operation, as shown in [5], convective and radiative heat loss from the device is negligible and heat dissipation is entirely due to the heat lost to the substrate by conduction through the base pads. This is modeled as a constant ambient temperature condition at the base pads as an essential boundary condition, EBC (see Fig. 5a), also known as Dirichlet boundary condition. However, this is not true when the thermal mass of the substrate is not large enough to maintain the ambient temperature. This can occur when a large array of electro-thermal devices are used as in [2] or when a device is thermally isolated from the substrate as shown in Fig. 6b. Then, a natural boundary condition, NBC (also known as Neumann boundary condition) must be imposed which leads to nonuniform temperature distribution at the base pad that will be known only after completing the thermal analysis.

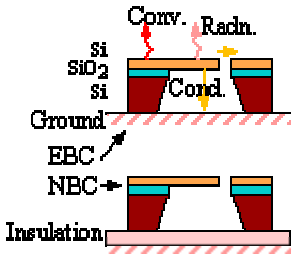

Fig. 6a A device for which an essential boundary condition is suitable

Fig. 6b A device for which a natural boundary condition is needed

3 COMPARISON OF EXPERIMENTAL AND SIMULATION DATA

3.1 Fabrication methods

Devices fabricated by MUMPs (μ-scale), PennSOIL [2] (micro and meso scales) and excimer laser micromachining (meso scale) are included in this study. In PennSOIL process, an silicon-on-insulator (SOI) wafer is etched on both sides to create deformable structures that are electrically insulated with each other. When the excimer laser is used, the micromachined device is bonded to an insulating material for testing. Some devices and several test structures were made using the above three processes. The resistance and deflection data for different applied voltages was obtained experimentally. See Figs. 7a through 7c for sample data.

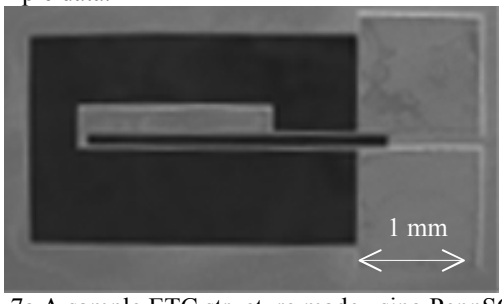

Fig. 7a A sample ETC structure made using PennSOIL

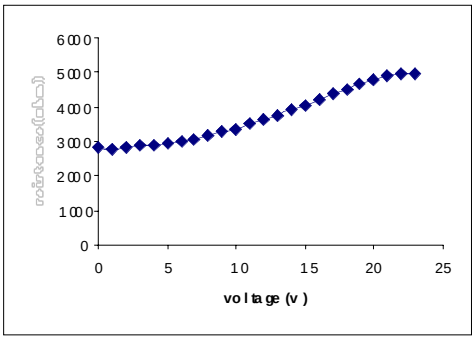

Fig. 7b Resistance vs. voltage data from the experiment

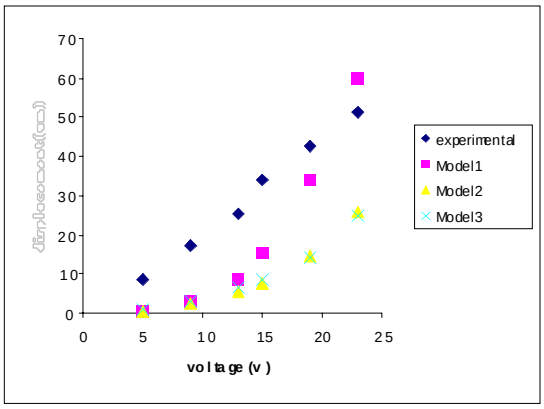

Fig. 7c Deflection vs. voltage of the device in Fig. 7a

3.2 Simulation

The sequential ETC simulation was performed in ABAQUS as well as using a simple analytical model using beam elements. Conduction through the substrate, conduction through the air gaps from the hot portion to the (relatively) cold portion, convection and radiation through all the exposed surfaces was included in the thermal analysis. Temperature dependent thermal conductivity [9] and coefficient of thermal expansion [10] along with the temperature, geometry and size dependent convection heat transfer coefficients [11] were used in simulating the ETC devices considered in this study. The following material property values at 300 K were used: Young's modulus = 169 GPa; Poisson's ratio = 0.3; thermal expansion coefficient = 2.5681E-06; thermal conductivity = 146 W/m-K; electrical conductivity = 2.857E4 /Ω-m.

Two sets of simulations were performed for devices of different sizes and different thermal boundary conditions (EBC and NBC). In the first set, the maximum temperature is kept the same for all simulations by applying appropriate voltage. In the second set, voltage was applied such that the energy input per second (power) is the same. It should be noted that when the device is in the steady state, all the energy input into the deflected device escapes as heat by way of conduction, convection, and radiation. The

consumption of this energy is necessary in order to retain the deflected state. The finite element model used in ABAQUS consisted of 3-D brick elements for the entire structure including the base pad. It was observed that considerable strain energy was stored in the base pads. So, in defining a reasonable output measure, the strain energy stored only in the "device" portion of the model (i.e., excluding the strain energy in the base pads) was used. The results of the simulations are given in Table 1 for the sample device of Fig. 7a. The *relative efficiency* shown in the table compares the ratio of the device strain energy to the energy input into the system per unit time at steady state. Micron sized device with the EBC was used in normalizing this performance parameter. The last row of the table shows the maximum disparity in the temperatures in the device, which is an approximate indicator of how well the nonuniform heating, has been achieved.

3.3 Observations

We found that the behavior of the devices under EBC and NBC conditions is significantly different (see Table 1). On the average, EBC devices run less hot, and NBC devices offer enhanced differential heating than the EBC devices, at both meso and micro scales. NBC devices offer higher operating efficiency ($energy_{out}/energy_{in}$) but suffer from large base pad strains under the same conditions. The relative efficiency defined above is used as the basis for comparing the device performance under EBC and NBC conditions. NBC devices have an overall superior performance at both scales for the same energy input. The meso scale devices operate at lower average temperatures and have significantly higher operating efficiencies than the micro scale ones for both types of thermal boundary conditions.

4 CONCLUSIONS

We note that in modeling the ETC devices, the thermal boundary condition can be either specified temperature (EBC) or specified (or unspecified) heat-flux (NBC). The fabrication method, packaging, and the environment of the device determine which boundary condition is appropriate. The choice of the type of boundary condition significantly affects the device behavior. Devices of micro and meso sizes, fabricated using different techniques, with EBC and NBC thermal boundary conditions are simulated and the results are compared. Based on the results, it appears that ETC actuation is more efficient at meso scale than micro scale.

ACKNOWLEDGMENTS

This research is supported by National Science Foundation grant (DMI-97-33916). The authors would like to Mr. Jun Li for his help in fabrication and testing of the devices.

5 REFERENCES

[1] Guckel, H., Klein, J., Christenson, T., Skrobis, K., Laudon, M., and Lovell, E.G., "Thermo-Magnetic Metal Flexure Actuators," Solid State Sensors and Actuators Workshop, Hilton Head Island, 1992, pp. 73-75.

[2] Comtois, J. and Bright, V., "Surface Micromachined Polysilicon Thermal Actuator Arrays and Applications," Hilton Head '96, p. 174.

[3] Moulton, T., "Analysis and Design of Electro-Thermal-Compliant Micro Devices," Center for Sensor Technologies at the University of Pennsylvania *technical report* # TR-CST31DEC97, pp. 13-26.

[4] Moulton, T. and Ananthasuresh, G.K., "Micromechanical Devices with Embedded Electro-Thermal-Compliant Actuation," *Micro-Electro-Mechanical Systems (MEMS) Symposium* at the IMECE 99.

[5] Lin, L. and Chiao, M., "Electrothermal Responses of Lineshape Microstructures," Sensors and Actuator A, 55, '96, pp. 35-41.

[6] Huang, Q. and Lee, N., "Analysis and Design of Polysilicon Thermal Flexure Actuator," J. Micromech. Microeng, 9, '98, pp. 64-70.

[7] Cragun, R. and Howell, L.L., "A Constrained Thermal Expansion Micro-Actuator," DSC-Vol. 66, *Micro-Electro-Mechanical Systems (MEMS) Symposium* at the IMECE 98, pp. 365-371.

[8] Guru, B.S. and Hiziroglu, H.R., 1997, *Electromagnetic Field Theory Fundamentals*, PWS Publishing Company, Boston.

[9] Touloukian, Y.S., "Thermophysical Properties of High Temperature of Solid Materials, Vol. 1, pp. 880.

[10] Okada, Y. and Tokumaru, Y., 1984, "Precise Determination of Lattice Parameter and Thermal Expansion Coefficient of Silicon Between 300 and 1500 K," J. Appl. Physics, 56 (2), 15 July, 1984, pp. 314-320.

[11] Mills, A. F., 1999, Basic Heat and Mass Transfer, Prentice Hall.

Table 1 Summary of effects of thermal boundary conditions and scale on a sample ETC device

	Comparison of performance for same max. temperature				Comparison of performance for same energy input			
	Meso/NBC	Micro/NBC	Meso/EBC	Micro/EBC	Meso/NBC	Micro/NBC	Meso/EBC	Micro/EBC
T_{max}	1451 K	1451 K	1451 K	1451 K	1451 K	1451 K	1336 K	1332 K
T_{min}	814 K	831 K	301 K	329 K	817 K	831 K	301 K	327 K
$Energy_{in}/sec$	424 mJ	32 mJ	490 mJ	37 mJ	424 mJ	32 mJ	424 mJ	32 mJ
Rel. effciency	121.43	1.42	97.86	1.14	121.43	1.42	85.7	1.0
$\overline{T}_{hot} - \overline{T}_{cold}$	442 K	435 K	453 K	415 K	442	434	397	374